

# Harnessing Geometric Constraints from Emotion Labels to Improve Face Verification

Anand Ramakrishnan, Minh Pham and Jacob Whitehill  
Worcester Polytechnic Institute

**Abstract**—For the task of face verification, we explore the utility of harnessing auxiliary facial emotion labels to impose explicit geometric constraints on the embedding space when training deep embedding models. We introduce several novel loss functions that, in conjunction with a standard Triplet Loss [43], or ArcFace loss [10], provide geometric constraints on the embedding space; the labels for our loss functions can be provided using either manually annotated or automatically detected auxiliary emotion labels. We analyze the performance of our methods on nine different (CK+, PubFig, Tufts, VggFace2, LFW, YTF, MegaFace, IJB-B, IJB-C). Our results consistently show that the additional structure encoded about each face’s emotions results in an embedding model that gives higher verification accuracy than training with just ArcFace or Triplet Loss alone. Moreover, the method is significantly more accurate than a simple multi-task learning approach. Our method is implemented purely in terms of the loss function and does not require any changes to the neural network backbone of the embedding function.

## I. INTRODUCTION

The goal of *face verification* is to determine automatically whether two face images belong to the same person. The state-of-the-art algorithms for face verification are based on embedding models that use deep convolutional neural networks (e.g., [43], [10], [50], [27]) to map face images into an embedding space such that multiple embeddings from the same person are close together and embeddings from different people are far apart. Deep embedding models can be used to measure the similarity between two inputs, even when they come from classes not seen during training. Current research in face verification is diverse, including equity in face verification accuracy [32], [51], [42], multimodal representations [2], [1], [45], 3-dimensional face verification, partial face verification [25], [13], [19], [12], loss function design [18], [43], [20], [10], large-scale datasets [6], [17], [8], and network architectures [5], [11].

**Contribution:** Our paper focuses on *harnessing auxiliary emotion label information* to construct an embedding space that can better explain the intra-class variance and thus better separate different classes (i.e., face IDs). Could training with these auxiliary labels result in a more accurate face verification system? To date, few works have investigated this question. In particular, we propose several novel geometry-constraining loss functions to encourage structure in the alignment of examples with the same face emotion labels by explicitly using either manually annotated or automatically detected emotion information. We show that harnessing this information helps obtain better-regularized embedding spaces (see Figure 1) and helps improve the performance on

the primary task of one-shot learning for face verification, relative to baseline models of Triplet Loss [43] and ArcFace loss [10]. To show the efficacy of our methods, we present results on nine face verification datasets. In contrast to *implicit* constraints on the embedding space via (for example) multi-task learning, we find that *explicit* constraints are more effective.

**Notation:** Let each example (face) be denoted by  $x$ . The embedding function  $f$  maps  $x$  into an embedding vector  $y$ . The one-shot class label (identity of the person) of  $x$  is denoted by  $c(x)$ , and the auxiliary label (facial expression) of  $x$  is denoted by  $e(x)$ .

## II. RELATED WORK

1) *Multi-Task Learning:* One prominent method of using auxiliary labels to improve generalization and obtain better latent representations is multi-task learning (MTL), an active field of literature for over 20 years [7]. Learning multiple tasks using a shared representation helps to regularize the model and improve its ability to generalize [40]. MTL has been successfully used in wide array of spaces including natural language processing [9], object detection [14], [39] and in drug discovery [38]. MTL can be interpreted as providing *implicit* structure on the embedding space to encourage better generalization; in contrast, our methods impose *explicit* structure on where different mini-clusters (corresponding to different auxiliary labels) within each cluster (face ID) should be located.

2) *Self Supervised Learning:* A promising new approach to learning representations of faces and other images is based on self-supervised learning [54], [44]. Self-supervision uses different proxy losses that enable it to learn suitable features for various downstream tasks. This is similar to an MTL setting, except the labels for the proxy losses are obtained through symmetry in the input data (e.g., the embeddings of face images from consecutive frames in a video should be very similar). Like MTL, the constraints imposed by self-supervision on the embedding space are *implicit*. In contrast, the loss functions we impose *explicit* constraints on the embedding space using auxiliary labels from either a human annotator or a pre-trained classifier of the auxiliary attributes.

3) *Auxiliary labels to improve embedding spaces:* [11] showed that including a wide variety of prediction tasks such as facial keypoint detection, face detection, etc., improves accuracy for the primary task of face verification. Fusing auxiliary information can help in speaker verification, as seen in [47]. [41] impose hierarchical priors using auxiliary

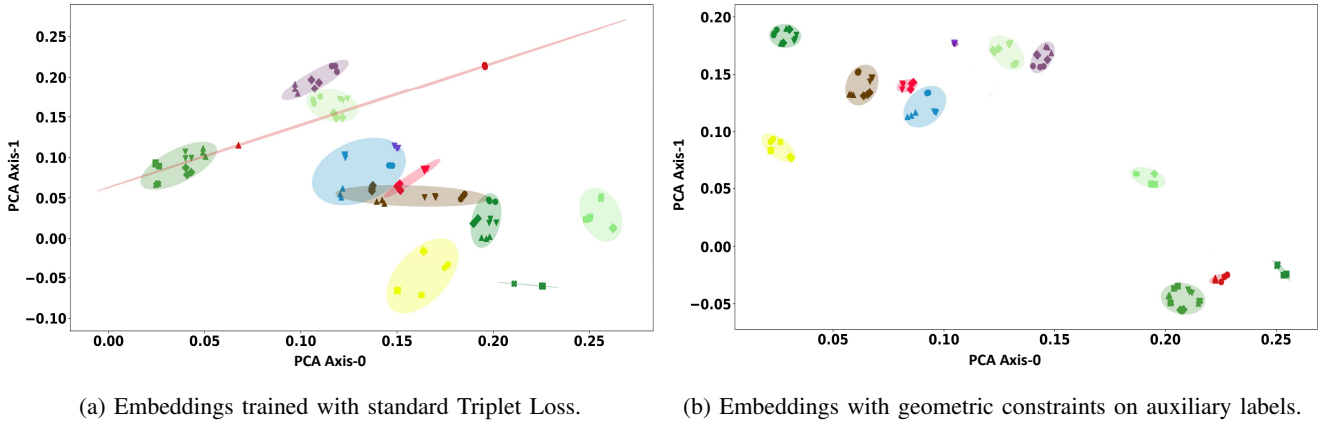


Fig. 1: PCA of the embeddings of the CK+ test data after training with (a) Triplet Loss, or (b) a combination of Triplet Loss and two additional novel loss functions ( $L_{PDP} + L_{FBV}$ ) that harness the auxiliary emotion labels. Color represents the one-shot class (face ID), and shapes represent the auxiliary information (facial expressions). By training with these extra loss terms, the clusters corresponding to one-shot classes become more regular and better separated.

labels to improve exponential-family embeddings and help in the primary task of capturing changes in word usage across different domains. The idea of hierarchical clusterings in the embedding space also inspired the PDM method presented in section III-C. The work most similar to our own is by [48], who propose a kernel-based constraint between image representations and auxiliary information. The authors obtain different auxiliary information (word embeddings, human annotations, etc.) and use deep kernel learning to construct an affinity kernel. The authors propose to maximize the relationship between the learned kernel and the corresponding embedding for the data. The PDP loss function proposed in section III-D is a looser form of this method.

4) *Euclidean vs. Spherical Embeddings*: Most prominent deep embedding models [43], [10], [56], [4], [15], [49] map their inputs into a hypersphere embedded in  $n$ -dimensional Euclidean space; these have the advantage that computing cosine similarity is trivial and that the distances between vectors are determined just based on their direction, not their lengths. However, embeddings into unconstrained Euclidean space are also possible and have been explored in the fields of word embeddings [30], image retrieval [34], [46] and face verification [36], [52]. In our work, we explore both spherical and Euclidean embeddings.

5) *Compositional Embeddings*: Recently there has been an interest in training neural networks to perform set operations (e.g., union) among multiple vectors in an embedding space to reflect higher-order relationships. Much of this work is for word embeddings [37], [33], [24]. However, a few works have also analyzed how embeddings of images with different class labels can be composed for multi-label one-shot learning. Both [26] and [3] present a compositional embedding model that can perform a different set of operations such as “contains”, “union”, etc., and achieves higher accuracy in multi-label one-shot learning tasks than traditional embedding methods. In one formulation [26], two embedding functions  $f$  and  $g$  are trained jointly:  $f$  embeds

an example (e.g., a face image) into the embedding space, whereas  $g$  maps from the embedding space to itself, to preserve certain relationships. While these methods utilize compositional models for multi-label one-shot learning, we extend this line of work by investigating how training  $f$  and  $g$  jointly can impose useful geometric constraints on the embedding space and help the model achieve higher accuracy for single-class one-shot learning.

### III. EXAMINED EMBEDDING METHODS

We propose new ways of improving the quality of embedding models by harnessing the geometric constraints imposed by emotion labels. We first describe the baseline approaches based on Triplet Loss and ArcFace loss functions. Then we propose several novel loss functions that impose additional geometric structure in the embedding space: Pairwise Distance Minimization (PDM), Pairwise Distance Preservation (PDP) (similar to [48]), Fixed Basis Vector (FBV), and Compositional Embeddings (CE) models.

#### A. Triplet Loss

A standard loss function for training an embedding model is the Triplet Loss (TL). Given three examples – the anchor  $x_a$ , a positive example  $x_p$  such that  $c(x_a) = c(x_p)$ , and a negative example  $x_n$  such that  $c(x_n) \neq c(x_a)$  – the loss is computed for each triplet as

$$L_{TL}(x_a, x_p, x_n) = \|f(x_a) - f(x_p)\|_2^2 - \|f(x_a) - f(x_n)\|_2^2 + \alpha \quad (1)$$

where  $\alpha \in \mathbb{R}$  is a margin hyperparameter. The Triplet Loss encourages examples from the same class to be close together and encourages examples from different classes to be far apart. In Figure 2, “No constraints” shows a hypothetical embedding space from such an approach: Colors represent different one-shot classes (e.g., face identities), and shapes represent auxiliary labels. There is no explicit incentive for the embedding function to organize the auxiliary labels in any systematic way.

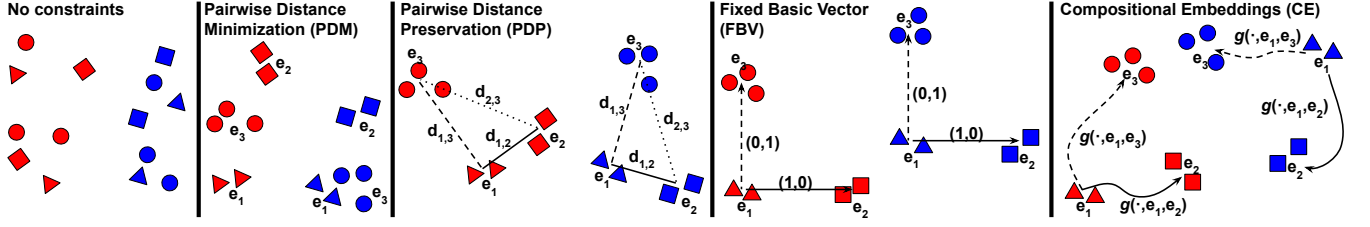


Fig. 2: The geometric constraints on auxiliary labels that we explore to improve face verification. Colors are one-shot classes (face identities); shapes are auxiliary labels (facial expression). With no constraints on embedding  $f$  beyond a standard Triplet/ArcFace Loss, the auxiliary labels within each one-shot class may be distributed arbitrarily. PDM pulls examples within each one-shot class having the same auxiliary label close together. PDP tries to maintain, over all one-shot classes, a fixed distance  $d_{a,b}$  between each *pair* of examples with the same one-shot class whose auxiliary labels are  $e_a$  and  $e_b$ , respectively. FBV is a stronger form of PDP: for each pair of auxiliary labels  $e_b \neq e_a$ , it fixes  $f(x_b) - f(x_a)$ , where  $e(x_b) = e_b$  and  $e(x_a) = e_a$ , to be a fixed vector. CE is a non-linear extension of FBV: using secondary function  $g$ , it estimates  $f(x_b)$  as  $g(f(x_a), e_a, e_b)$ .

### B. ArcFace Loss

The ArcFace loss as proposed in [10] has achieved state-of-the-art results in various benchmark datasets. ArcFace inserts an angular margin geodesic distance between the sample and centers. ArcFace is based on the loss function

$$L_{\text{AF}}(x_a, \bar{x}_p, \bar{x}_n) = \text{GDis}(f(x_a), f(\bar{x}_p)) - \text{GDis}(f(x_a), f(\bar{x}_n)) + \alpha$$

where GDis is the geodesic distance (arc length) between two points embedded on a sphere, and  $\bar{x}_p, \bar{x}_n$  are the centroids of the embeddings for persons  $x_p$  (where  $c(x_p) = c(x_a)$ ) and  $x_n$  (where  $c(x_n) \neq c(x_a)$ ), respectively.

### C. Pairwise Distance Minimization

The first method we explored for enforcing more geometric structure on the embedding space using the auxiliary labels is the Pairwise Distance Minimization (PDM) Loss. It encourages all examples within each one-shot class that has the same auxiliary label to be close together. In this way, the PDM encourages the formation of “mini-clusters” within each one-shot cluster. One can thus view this loss function as a form of hierarchical clustering. Figure 2 illustrates this idea. Given two examples:  $x_a$  and  $x_b$  such that  $c(x_a) = c(x_b)$  and  $e(x_a) = e(x_b)$ , the PDM loss is computed for each pair:

$$L_{\text{PDM}}(x_a, x_b) = \|f(x_a) - f(x_b)\|_2^2 \quad (2)$$

We note that in contrast to multi-task learning (MTL) (see Section III-G) that defines *implicit* relationships between embedding function and the emotion labels, PDM defines an *explicit* relationship between the embedding representation and the auxiliary labels by imposing constraints on the loss function. Such explicit constraints may provide a better embedding space for one-shot learning compared to MTL.

### D. Pairwise Distance Preservation

In the PDM loss we only explicitly encouraged the model to form clusters for *individual* emotion labels. However, imposing constraints on how the multiple mini-clusters corresponding to different auxiliary labels should align with each

other in the embedding space might help to better regularize the model. With the Pairwise Distance Preservation (PDP) loss we propose to encourage our model to maintain the same distance *between* two auxiliary clusters across all one-shot classes. As shown in Figure 2, we want auxiliary clusters corresponding to auxiliary labels  $e_1$ ,  $e_2$ , and  $e_3$  to have a similar distance across all one-shot classes. Given four examples:  $x_1, x_2, x_3$  &  $x_4$  such that  $c(x_1) = c(x_2)$ ,  $c(x_3) = c(x_4)$ ,  $c(x_1) \neq c(x_3)$  and  $e(x_1) = e(x_3)$ ,  $e(x_2) = e(x_4)$ ,  $e(x_1) \neq e(x_2)$ , the PDP loss is computed for each quadruple:

$$L_{\text{PDP}}(x_1, x_2, x_3, x_4) = (\|f(x_1) - f(x_2)\|_2^2 - \|f(x_3) - f(x_4)\|_2^2)^2 \quad (3)$$

### E. Fixed Basis Vector Separation

With the PDP loss, we encourage the embedding space to generate mini-clusters based on the auxiliary labels with similar distances, but the relative positions of the mini-cluster centroids could still vary from one person to another. In contrast, the Fixed Basis Vector (FBV) loss that we propose forces the auxiliary clusters to align along a particular fixed vector across all the one-shot classes. In particular, we select one auxiliary class  $e_1$  (say, a Neutral facial expression) as the “origin” each one-shot class. Then, for each other auxiliary label, we choose a unique Euclidean basis vector in the embedding space (e.g.,  $(1, 0, \dots, 0)$  for Neutral to Anger, or  $(0, 1, 0, \dots, 0)$  for Neutral to Sadness) as the desired vector between pairs of mini-clusters. In general, given two examples  $x_a, x_b$  such that  $c(x_a) = c(x_b)$ ,  $e(x_a) \neq e(x_b)$ , and  $v_{ab}$  is the unique fixed basis vector for the emotion pair  $(e_a, e_b)$ , the FBV loss is computed for the pair as

$$L_{\text{FBV}}(x_a, x_b) = \|f(x_b) - f(x_a) - v_{ab}\|_2^2 \quad (4)$$

One can also view the FBV loss as a combination of PDM and a stronger PDP since the FBV loss forces the individual auxiliary clusters to be close to each other.

Importantly, when using the FBV loss, we remove the constraint – which is commonplace with Triplet Loss and required for ArcFace loss – that the embedding vectors must

lie on a hypersphere. Instead, each embedding  $y$  can be any point in Euclidean space.

#### F. Compositional Embedding

The FBV loss encourages  $f$  to organize the embedded examples such that, for each one-shot class, the mini-cluster corresponding to  $e_b$  can be reached from the mini-cluster corresponding to  $e_a$  simply by adding a fixed basis vector  $v_{ab}$ . However, there may be other *non-linear* mappings from one mini-cluster to another that more faithfully model the data and thereby yield an embedding space that separates the one-shot classes more accurately. With this goal in mind, we expand on the idea of *compositional embeddings* ([3]; [26]) by introducing a compositional model  $g$  to learn a non-linear map from one auxiliary mini-cluster to another in the embedding space. Through a joint training procedure,  $g$  forces  $f$  to align the auxiliary mini-clusters to be separable within each one-shot class while also potentially increasing the separability of the one-shot clusters themselves.

Suppose  $x_a$  and  $x_b$  are two examples from the same person that have different auxiliary labels, i.e.,  $c(x_a) = c(x_b)$ ,  $e(x_a) \neq e(x_b)$ . We define our composition function  $g$  and train it using the loss

$$L_{CE}(x_a, x_b) = \|g(f(x_a), e(x_a), e(x_b)) - f(x_b)\|_2^2 \quad (5)$$

This encourages  $g$  to estimate  $f(x_b)$  based on  $f(x_a)$  and the auxiliary labels of these two examples. The CE method simplifies to FBV if we let  $g(f(x_a), e(x_a), e(x_b)) = f(x_a) + v_{ab}$  for some fixed  $v_{ab}$ . In our implementation,  $g$  consists of a 3 layer fully connected network (FCN(100)-ReLU-FCN(100)-ReLU-FCN(100)).

#### G. Multitask Learning

One of the simplest methods to harness auxiliary information for improving latent representations is multi-task learning (MTL). Here, a single common latent layer is used to model multiple target variables (face identity and facial expression). The intuition for this idea is that training on multiple tasks helps to regularize the convolution layers, which could help perform better at the primary task of one-shot learning.

In our experiments, we implement MTL as a baseline for comparison. In a pilot testing experiment, we tried adding a classification head directly after the final embedding layer that takes the embedding vector as input and predicts the auxiliary label (the facial expression of a person's face image) as output. We found that this method resulted in an overall decrease in face verification accuracy. Instead, we found that branching into two separate tasks immediately after the last convolution layer helped improve the model's accuracy. In particular, the classification head is a 3-layer network with softmax output: FCN(100)-ReLU-FCN(100)-ReLU-FCN(Classes)-SoftMax.

### IV. EXPERIMENTS

We conducted experiments to assess to what extent the proposed loss functions – PDM, PDP, FBV, and CE – may

improve upon a Triplet Loss and ArcFace loss as well as MTL as baselines. In particular, we compare training with  $L_{TL}$  or  $L_{AF}$ , to training with one of these loss functions combined with one (or several) of the proposed loss functions (e.g.,  $L_{TL} + L_{PDP}$ ). We found that weighting both (or all) the loss functions equally gave good results in pilot experiments, and we did not optimize this hyperparameter extensively.

We apply one-shot learning to the task of face verification: given a trained embedding model  $f$ , and given a face image  $x$ , the task is to determine, for a query face  $x_q$ , whether it contains the same ( $c(x) = c(x_q)$ ) or a different ( $c(x) \neq c(x_q)$ ) person as  $x$ . For evaluation we utilize multiple metrics dependent on the dataset (see section IV-A). In particular, we provide True Acceptance Rate at False Acceptance Rate threshold of  $1e-4$  or  $1e-6$  and the Mean Accuracy for correctly classifying each pair of examples in the test set from the same one-shot class (face ID) versus different one-shot classes. We also perform several follow-up analyses to understand the differences in accuracy that we observe.

Note that, when training with ArcFace loss, we found that we could not achieve the same accuracies as reported in [10] when trained from scratch using the provided GitHub repository [16]. Hence, we present the results on the different datasets as obtained by our trained model from scratch in Table I (row 8).

#### A. Datasets (Training & Testing)

We compare the different embedding loss functions on several well-known face datasets:

1) *CK+*: The Cohen Kanade Plus dataset (CK+) [28] contains 981 images and 123 unique face IDs. 80 IDs were randomly selected for training, and the remaining 43 IDs for testing. The 80 training IDs were further divided into 60 IDs for training and 20 IDs as validation. The CK+ dataset includes posed emotion labels for all the images with the different categories being “Happy”, “Sadness”, “Anger”, “Surprise”, “Fear”, “Disgust”.

2) *Tufts*: The Tufts face database [35] is a multimodal face dataset with 113 IDs in total and images in different modes such as color, pencil sketch, 3D, thermal, etc., from which we only utilize the visible color images. 80 IDs were randomly selected for training, and the remaining 33 IDs for testing. The 80 training IDs were further divided into 60 IDs for training and 20 IDs as validation. The Tufts face dataset includes five auxiliary labels (e.g., “smile”, “open mouth”) that we use for training the proposed loss functions.

3) *PubFig Dataset*: The Public Figures dataset [23] is a large real-world dataset with 200 IDs and 58797 Images. PubFig is divided into a development set with 60 IDs and 16,336 images and an evaluation set with 140 IDs and 42,641 images. The 60 IDs in the development set are used for training and are further divided into 45 IDs for training and 15 IDs for validation. The evaluation dataset is used as the test dataset.

4) *VGGFace2*: The VGGFace2 dataset [6] is a challenging large-scale face verification dataset with around 9000 IDs and over 3.3 million images with about 362 images per ID. The dataset is divided into 8631 IDs for training and 500 IDs as the test dataset. The 8631 training IDs were further divided into 4000 IDs for training and 2631 IDs as validation.

For the above four datasets, we evaluate the results on the test datasets by providing the  $\text{TAR}(@\text{FAR}=1\text{e-}4)$  values, i.e., the True Acceptance Rate when the False Acceptance Rate is fixed to  $1\text{e-}4$ .

### B. Benchmark Datasets (Testing Only)

To evaluate our methods and compare them with existing results, we evaluate on five benchmark datasets that are used only for *evaluating* our models; for *training* our models, we thus use a different dataset – MS1MV2 dataset, a semi-automatic refined version of MS-Celeb-1M dataset [17]. Below we describe each evaluation dataset.

1) *Labeled Faces in the Wild (LFW)*: The LFW dataset [21] is an unconstrained dataset consisting of 5749 IDs and 13233 images with non-frontal faces. We report the mean classification accuracy for the pairs of images similar to [43]. We follow the unrestricted with labeled outside data protocol to report the performance. We report the mean classification accuracy for the pair of images similar to [43].

2) *Youtube Faces (YTF)*: The YTF dataset [55] is a dataset of unconstrained face videos containing 3,425 videos of 1,595 different people. An average of 2.15 videos is available for each subject. The shortest clip duration is 48 frames, the longest clip is 6,070 frames, and the average length of a video clip is 181.3 frames. We follow the unrestricted with labeled outside data protocol to report the performance. We report the mean classification accuracy for the pairs of videos similar to [43].

3) *MegaFace*: The MegaFace dataset [22] includes 1,000,000 images with around 69000 IDs as the gallery set and around 100,000 images of 530 IDs as the probe set. We report the verification accuracy on the MegaFace Challenge 1 using Facescrub as the probe dataset. We report the  $\text{TAR}(@\text{FAR}=1\text{e-}6)$  to evaluate the results similar to [10].

4) *IJB-B*: The IJB-B dataset [53] contains 1845 IDs with around 67,000 face images and 10,000 nonface images from around 7000 videos. We report the  $\text{TAR}(@\text{FAR}=1\text{e-}4)$  to evaluate the results similar [10].

5) *IJB-C*: The IJB-C dataset [29] is an extension of the IJB-B dataset and contains 3,531 IDs with 138,800 face images and 10,000 nonface images from around 11,000 videos. We report the  $\text{TAR}(@\text{FAR}=1\text{e-}4)$  to evaluate the results similar [10].

To compute the embeddings for video datasets (IJB-B, IJB-C, and YTF), we calculate the mean embedding of all frames from the video similar to [10].

**Emotion Detector**: VGGFace2, PubFig, and MS1MV2 datasets contain no human-annotated emotion labels. Hence, to estimate the auxiliary emotion labels for these datasets, we trained a custom emotion detector using a Resnet-50 model on the AffectNet dataset [31]. The AffectNet dataset is a

large-scale facial expression dataset. The model is trained for a 7-way categorical classification task (“Happy”, “Sadness”, “Anger”, “Surprise”, “Fear”, “Disgust”, “Neutral”) on a training dataset of size 100,000 for 100 epochs with Adam as the optimizer and a learning rate of 0.001. A validation dataset of size 10,000 is used, and early stopping is employed with patience of 25 epochs based on the validation loss. The best-trained model based on the validation loss is then used to predict the emotion labels on the datasets. These labels are used as the auxiliary labels for our methods.

### C. Training Procedure

All faces are cropped and aligned using MTCNN [57] and resized to 100x100. We use the Inception-Resnet-V1 as the embedding model backbone (as described in [43]) for the Triplet Loss model and the Resnet-100 architecture (as described in [10]) for the ArcFace loss models. The output embedding space in our models is either spherical or Euclidean based on the nature of the secondary loss function, and the output is a 512-dimensional vector. All models are trained with a batch size of 128. Early stopping based on the validation Triplet/ArcFace loss with patience of 10 epochs is employed, and the best model based on validation loss is used as the final model. Adam is used as the optimizer with a learning rate of 0.001.

1) *HyperParameters*: For the Triplet Loss-based models, we use data generators to randomly create our training data in triplets using the training ID set and create our validation dataset from the validation ID set. For loss parameters, we utilize a margin distance of  $\alpha = 1.0$  for all the spherical models and a margin distance of 5.0 for the Euclidean models (In a pilot test, we tuned for the margin distance and found this distance to work best.)

For ArcFace we set the feature scale  $s=64$  as defined in [50] and utilize a margin value  $\alpha = 0.5$  as defined in [10].

Finally, we set the fixed basis vector distance in the FBV secondary loss to be 1.0.

## V. RESULTS

Table I shows the results for the different datasets (for face verification) for the different embedding losses.

The best results for all datasets were achieved using ArcFace Loss (AF) with PDP and FBV using a Euclidean embedding space and the Resnet-100 CNN backbone. The combination  $L_{\text{AF}} + L_{\text{PDP}} + L_{\text{FBV}}$  provided an accuracy boost compared to training on the ArcFace loss alone and compared to training with ArcFace using multi-task learning (MTL). Moreover, the same trend persisted when training with the Triplet Loss with an Inception-Resnet backbone.

Below we discuss specific trends:

1) *Comparison with TL*: We found a consistent accuracy improvement for all datasets with *each* of the proposed loss functions (PDM, PDP, FBV, and CE) compared to training with Triplet Loss (TL) alone (row 1). The *combination* of PDP and FBV, together with TL, was also particularly effective. To see whether the accuracy using TL loss alone could be improved simply by varying the margin  $\alpha$ , we tried

Accuracy vs Embedding Methods															
#	Methods						Datasets								
	Base	MTL	PDM	PDP	FBV	CE	TAR @ FAR=1e-4					Mean Accuracy		TAR @ FAR=1e-6	
							CK+	Tufts	PubFig	VGGFace2	IJB-B	IJB-C	LFW	YTF	MegaFace
1.	TL						0.913	0.921	0.769	0.754	0.805	0.847	0.988	0.911	0.887
2.	TL	✓					0.922	0.929	0.777	0.761	0.812	0.859	0.990	0.919	0.893
3.	TL		✓				0.918	0.927	0.782	0.772	0.811	0.858	0.990	0.920	0.899
4.	TL			✓			0.934	0.932	0.783	0.777	0.819	0.861	0.991	0.922	0.903
6.	TL		✓		✓		0.939	0.934	0.788	0.783	0.838	0.873	0.991	0.928	0.910
7.	TL			✓	✓		<b>0.943</b>	<b>0.938</b>	<b>0.790</b>	<b>0.789</b>	<b>0.852</b>	<b>0.878</b>	<b>0.992</b>	<b>0.931</b>	<b>0.914</b>
8.	TL					✓	0.931	0.928	0.784	0.777	0.833	0.863	0.991	0.923	0.902
9.	AF						0.963	0.951	0.864	0.853	0.891	0.899	0.994	0.950	0.951
10.	AF	✓					0.966	0.953	0.864	0.854	0.895	0.901	0.993	0.949	0.952
11.	AF		✓				0.968	0.949	0.863	0.844	0.913	0.921	0.992	0.949	0.952
12.	AF			✓			0.973	0.953	0.864	0.846	0.927	0.933	0.993	0.953	0.953
14.	AF		✓		✓		0.975	0.957	0.871	0.868	0.931	0.938	0.994	0.958	0.954
15.	AF			✓	✓		<b>0.980</b>	<b>0.958</b>	<b>0.874</b>	<b>0.871</b>	<b>0.947</b>	<b>0.950</b>	<b>0.995</b>	<b>0.961</b>	<b>0.958</b>
16.	AF					✓	0.974	0.939	0.870	0.859	0.918	0.929	0.993	0.952	0.954

TABLE I: Accuracy of the different constraint-based embedding methods on the nine different datasets. Base indicates whether Triplet Loss or ArcFace loss is used. For the former, an Inception-Resnet is used as the backbone; for the latter, a Resnet-100 is used. The checkmarks indicate the additional loss functions that are added during training. When training with the FBV loss, the model embeds the face images into Euclidean space; otherwise, it embeds into a hypersphere.

re-training and evaluating using a range of values between 0.1 and 1.0 but did not find any improvement.

#### A. Comparison with ArcFace

Using ArcFace in conjunction with  $L_{PDM} + L_{FBV}$ , or in conjunction with  $L_{PDP} + L_{FBV}$ , consistently delivered better accuracy than training with ArcFace alone (row 8).

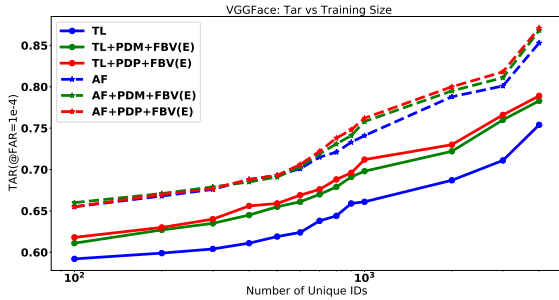


Fig. 3: Tar(@Far=1e-4) values on the VGGFace Test dataset as a function of Training dataset size in log scale.

1) *Comparison with MTL*: Adding the MTL layer provides a consistent increase in accuracy over plain TL (row 2). We also see a slight increase in accuracy over plain ArcFace except on the LFW and YTF datasets (row 9). However, MTL was not as effective as the addition of both PDP and FBV.

2) *Pairwise Distance Minimization*: Adding the PDM loss provides a consistent increase over plain TL over all the datasets (row 3) but not over the plain ArcFace loss (row 10).

3) *Pairwise Distance Preservation*: Replacing PDM with PDP loss improves the model’s performance on all the datasets over plain Triplet Loss (row 4). We also see a slight boost on adding PDP loss over plain AF loss (row 11). The improvement in the model’s performance suggests

that more rigorous constraints that impose more structure on the embedding space produce better results on the face verification task.

4) *Fixed Basis Vector*: In pilot experiments (not shown), we found that adding FBV loss to TL and AF by itself did not produce good results. Instead, including FBV loss *and* either PDM or PDP loss improved the model’s performance compared to just PDM or PDP over both TL and AF (row 5, 6, 12 & 13). One possible theory why the FBV loss works best in tandem with the other losses is that the auxiliary labels’ cluster centers are initially ill-defined. Adding PDM/PDP provides an additional incentive to form clusters, thus helping the FBV loss. AF+PDP+FBV is the best performing model on the face verification task across all the datasets (row 13).

5) *Compositional Embeddings*: The Compositional Embedding loss was competitive with but no better than the other loss functions we proposed (row 7 & 14). In other words, we found no support for the hypothesis that non-linear mappings from one auxiliary mini-cluster to another are essential for the primary task of one-shot classification.

#### B. Euclidean versus Spherical Embeddings

We find that embedding into Euclidean space gives not only more flexibility in the output of the embedding function  $f$  but can also help it to achieve higher accuracy. In particular, the FBV loss variants require a Euclidean embedding space. However, without the FBV loss, the unconstrained Euclidean embeddings did not work: The plain Triplet Loss embedding model that mapped into unconstrained Euclidean space performed poorly compared to mapping into the hypersphere – the TAR(@FAR=1e-4) scores were 0.81, 0.85, 0.69, and 0.65 on the CK+, Tufts, PubFig, and VGGFace2 datasets respectively.



## VI. ADDITIONAL EXPERIMENTS

We conducted additional experiments to understand better the accuracy gains described in the previous section.

### A. Alternative Hypotheses

One alternative hypothesis to explain our results is that the improved model performance might have nothing to do with the geometric constraints; instead, the boost in performance might result from a stronger gradient from the loss functions or tuning an important hyperparameter such as the margin. We performed the following experiment to explore this hypothesis: We shuffled the auxiliary information present among its images and then retrained the embedding models for all the face IDs in the training set. We obtained the following results when we use the AF+PDP+FBV as the loss function: TAR(@FAR=1e-4) values of 0.962, 0.951, 0.864, 0.852, 0.892, and 0.899 for CK+, Tufts, PubFig, VGGFace2, IJB-B, and IJB-C datasets, respectively, Mean accuracy of 0.990 and 0.944 for LFW and YTF datasets respectively and TAR(@FAR=1e-6) value of 0.941 for MegaFace. The model's performance is substantially worse than with genuine auxiliary labels and is comparable with the performance of the plain ArcFace Loss model across all datasets. This suggests that the gains achieved are due to the utilization of the structure defined by the auxiliary label.

### B. Training Size vs. Accuracy

To explore how the benefits of the additional loss functions may change as a function of the training set size, we explored on the VGGFace2 dataset how reducing the number of unique face IDs in the training set impacts the accuracy gained using the different geometric constraints. Figure 3 shows the TAR(@FAR=1e-4) versus the training set size. The PDP+FBV, in conjunction with either TL or ArcFace, is consistently the best model over all training set sizes we tried. The advantage of harnessing the additional geometric structure afforded by the auxiliary emotion labels does not diminish with training set size, suggesting that they can be worthwhile even when many unique face IDs are available.

### C. Detected Emotions vs True Emotions

In some training datasets used for one-shot learning, auxiliary labels may exist but might not be labeled. Can we obtain similar accuracy gains as we observed in our experiments using labels generated from an automatic classifier? In a final experiment, we show the different loss functions' results on the CK+ dataset using the detected emotions in table II. Comparing the results from table II with the results on the CK+ dataset in table I we see that the accuracy gain from the proposed loss functions is diminished, relative to using human-annotated labels, but still definitely present compared to just the TL loss.

## VII. CONCLUSION

We have presented several novel loss functions that impose geometrical constraints, based on emotion labels, on the embedding models used for face verification. We illustrated how

CK+ Detected Emotion Results	
Method	TAR(@FAR=1e-4)
TL+MTL	0.919
TL+PDM	0.916
TL+PDP	0.930
TL+PDM+FBV	0.935
TL+PDP+FBV	0.936
TL+CE	0.925

TABLE II: TAR scores using detected rather than human-annotated auxiliary labels on the CK+ Dataset.

they help improve face verification performances on widely used datasets (CK+, TUfts Face DB, PubFig, VGGFace2, IJB-B, IJB-C, LFW, YTF, and MegaFace).

Our experiments yielded several noteworthy results: (1) Imposing stricter geometric structure on the embedding space based on auxiliary labels improves one-shot verification accuracy substantially, and its utility surpasses that of multi-task learning. The most substantial accuracy gains are derived from combining both FBV and PDP losses. (2) Harnessing the auxiliary labels to provide geometric structure can be effective, albeit to diminished effect, using automatically detected labels rather than human-annotated labels. (3) Compared to using spherical embedding space, the Euclidean embedding space is more flexible and yields higher accuracy, provided the loss function imposes enough geometric structure. (4) The additional loss functions can be effective in small and large training set regimes.

We note that, while we explored the utility of the proposed loss functions for the auxiliary task of *emotion*, we could also explore their utility for other face attributes such as age, head pose, etc. Finally, we note that the ideas presented here are not limited to face-verification and could be used in any few-shot learning task when auxiliary labels are available.

## REFERENCES

- [1] A. S. Al-Waisy, S. Al-Fahdawi, and R. Qahwaji. A multi-biometric face recognition system based on multimodal deep learning representations. *Deep Learning in Computer Vision; Informa UK Limited: Colchester, UK*, pages 89–126, 2020.
- [2] A. S. Al-Waisy, R. Qahwaji, S. Ipson, and S. Al-Fahdawi. A multimodal deep learning framework using local feature representations for face recognition. *Machine Vision and Applications*, 29(1):35–54, 2018.
- [3] A. Alfassy, L. Karlinsky, A. Aides, J. Shtok, S. Harary, R. Feris, R. Giryes, and A. M. Bronstein. Laso: Label-set operations networks for multi-label few-shot learning. In *Proceedings of the IEEE Conference on Computer Vision and Pattern Recognition*, pages 6548–6557, 2019.
- [4] A. Banerjee, I. S. Dhillon, J. Ghosh, and S. Sra. Clustering on the unit hypersphere using von mises-fisher distributions. *Journal of Machine Learning Research*, 6(Sep):1345–1382, 2005.
- [5] K. Cao, Y. Rong, C. Li, X. Tang, and C. Change Loy. Pose-robust face recognition via deep residual equivariant mapping. In *Proceedings of the IEEE Conference on Computer Vision and Pattern Recognition*, pages 5187–5196, 2018.
- [6] Q. Cao, L. Shen, W. Xie, O. M. Parkhi, and A. Zisserman. Vggface2: A dataset for recognising faces across pose and age. In *2018 13th IEEE International Conference on Automatic Face & Gesture Recognition (FG 2018)*, pages 67–74. IEEE, 2018.
- [7] R. Caruana. Multitask learning. *Machine learning*, 28(1):41–75, 1997.
- [8] J. S. Chung, A. Nagrani, and A. Zisserman. Voxceleb2: Deep speaker recognition. *arXiv preprint arXiv:1806.05622*, 2018.
- [9] R. Collobert and J. Weston. A unified architecture for natural language processing: Deep neural networks with multitask learning. In

- Proceedings of the 25th international conference on Machine learning*, pages 160–167, 2008.
- [10] J. Deng, J. Guo, N. Xue, and S. Zafeiriou. Arcface: Additive angular margin loss for deep face recognition. In *Proceedings of the IEEE Conference on Computer Vision and Pattern Recognition*, pages 4690–4699, 2019.
  - [11] J. Deng, J. Guo, Y. Zhou, J. Yu, I. Kotsia, and S. Zafeiriou. Retinaface: Single-stage dense face localisation in the wild. *arXiv preprint arXiv:1905.00641*, 2019.
  - [12] Y. Duan, J. Lu, J. Feng, and J. Zhou. Topology preserving structural matching for automatic partial face recognition. *IEEE Transactions on Information Forensics and Security*, 13(7):1823–1837, 2018.
  - [13] A. Elmahmudi and H. Ugail. Deep face recognition using imperfect facial data. *Future Generation Computer Systems*, 99:213–225, 2019.
  - [14] R. Girshick. Fast r-cnn. In *Proceedings of the IEEE international conference on computer vision*, pages 1440–1448, 2015.
  - [15] S. Gopal and Y. Yang. Von mises-fisher clustering models. In *International Conference on Machine Learning*, pages 154–162, 2014.
  - [16] J. Guo and J. Deng. Arcface: Additive angular margin loss for deep face recognition. <https://github.com/deepinsight/insightface>, 2019.
  - [17] Y. Guo, L. Zhang, Y. Hu, X. He, and J. Gao. Ms-celeb-1m: A dataset and benchmark for large-scale face recognition. In *European conference on computer vision*, pages 87–102. Springer, 2016.
  - [18] R. Hadsell, S. Chopra, and Y. LeCun. Dimensionality reduction by learning an invariant mapping. In *2006 IEEE Computer Society Conference on Computer Vision and Pattern Recognition (CVPR'06)*, volume 2, pages 1735–1742. IEEE, 2006.
  - [19] L. He, H. Li, Q. Zhang, and Z. Sun. Dynamic feature learning for partial face recognition. In *Proceedings of the IEEE conference on computer vision and pattern recognition*, pages 7054–7063, 2018.
  - [20] A. Hermans, L. Beyer, and B. Leibe. In defense of the triplet loss for person re-identification. *arXiv preprint arXiv:1703.07737*, 2017.
  - [21] G. B. Huang, M. Mattar, T. Berg, and E. Learned-Miller. Labeled faces in the wild: A database for studying face recognition in unconstrained environments. In *Workshop on faces in 'Real-Life' Images: detection, alignment, and recognition*, 2008.
  - [22] I. Kemelmacher-Shlizerman, S. M. Seitz, D. Miller, and E. Brossard. The megaface benchmark: 1 million faces for recognition at scale. In *Proceedings of the IEEE conference on computer vision and pattern recognition*, pages 4873–4882, 2016.
  - [23] N. Kumar, A. C. Berg, P. N. Belhumeur, and S. K. Nayar. Attribute and simile classifiers for face verification. In *2009 IEEE 12th international conference on computer vision*, pages 365–372. IEEE, 2009.
  - [24] B. Lake and M. Baroni. Generalization without systematicity: On the compositional skills of sequence-to-sequence recurrent networks. In *International Conference on Machine Learning*, pages 2873–2882. PMLR, 2018.
  - [25] Y. Lei, Y. Guo, M. Hayat, M. Bennamoun, and X. Zhou. A two-phase weighted collaborative representation for 3d partial face recognition with single sample. *Pattern Recognition*, 52:218–237, 2016.
  - [26] Z. Li, M. Mozer, and J. Whitehill. Compositional embeddings for multi-label one-shot learning. *arXiv preprint arXiv:2002.04193*, 2020.
  - [27] W. Liu, Y. Wen, Z. Yu, M. Li, B. Raj, and L. Song. Sphereface: Deep hypersphere embedding for face recognition. In *Proceedings of the IEEE conference on computer vision and pattern recognition*, pages 212–220, 2017.
  - [28] P. Lucey, J. F. Cohn, T. Kanade, J. Saragih, Z. Ambadar, and I. Matthews. The extended cohn-kanade dataset (ck+): A complete dataset for action unit and emotion-specified expression. In *2010 IEEE computer society conference on computer vision and pattern recognition-workshops*, pages 94–101. IEEE, 2010.
  - [29] B. Maze, J. Adams, J. A. Duncan, N. Kalka, T. Miller, C. Otto, A. K. Jain, W. T. Niggel, J. Anderson, J. Cheney, et al. Iarpa janus benchmark-c: Face dataset and protocol. In *2018 International Conference on Biometrics (ICB)*, pages 158–165. IEEE, 2018.
  - [30] T. Mikolov, K. Chen, G. Corrado, and J. Dean. Efficient estimation of word representations in vector space. *arXiv preprint arXiv:1301.3781*, 2013.
  - [31] A. Mollahosseini, B. Hasani, and M. H. Mahoor. Affectnet: A database for facial expression, valence, and arousal computing in the wild. *IEEE Transactions on Affective Computing*, 10(1):18–31, 2017.
  - [32] S. Nagpal, M. Singh, R. Singh, and M. Vatsa. Deep learning for face recognition: Pride or prejudiced? *arXiv preprint arXiv:1904.01219*, 2019.
  - [33] P. Nakov, A. Ritter, S. Rosenthal, F. Sebastiani, and V. Stoyanov. Semeval-2016 task 4: Sentiment analysis in twitter. *arXiv preprint arXiv:1912.01973*, 2019.
  - [34] H. Oh Song, Y. Xiang, S. Jegelka, and S. Savarese. Deep metric learning via lifted structured feature embedding. In *Proceedings of the IEEE conference on computer vision and pattern recognition*, pages 4004–4012, 2016.
  - [35] K. Panetta, Q. Wan, S. Agaian, S. Rajeev, S. Kamath, R. Rajendran, S. P. Rao, A. Kaszowska, H. A. Taylor, A. Samani, and X. Yuan. A comprehensive database for benchmarking imaging systems. *IEEE Transactions on Pattern Analysis and Machine Intelligence*, 42(3):509–520, 2020.
  - [36] O. Parkhi, A. Vedaldi, and A. Zisserman. Deep face recognition. In *BMVC*, 2015.
  - [37] J. B. Pollack. Implications of recursive distributed representations. In *Advances in neural information processing systems*, pages 527–536, 1989.
  - [38] B. Ramsundar, S. Kearnes, P. Riley, D. Webster, D. Konerding, and V. Pande. Massively multitask networks for drug discovery. *arXiv preprint arXiv:1502.02072*, 2015.
  - [39] S. Ren, K. He, R. Girshick, and J. Sun. Faster r-cnn: Towards real-time object detection with region proposal networks. In *Advances in neural information processing systems*, pages 91–99, 2015.
  - [40] S. Ruder. An overview of multi-task learning in deep neural networks. *arXiv preprint arXiv:1706.05098*, 2017.
  - [41] M. Rudolph, F. Ruiz, S. Athey, and D. Blei. Structured embedding models for grouped data. In *Advances in neural information processing systems*, pages 251–261, 2017.
  - [42] H. J. Ryu, H. Adam, and M. Mitchell. Inclusivefacenet: Improving face attribute detection with race and gender diversity. *arXiv preprint arXiv:1712.00193*, 2017.
  - [43] F. Schroff, D. Kalenichenko, and J. Philbin. Facenet: A unified embedding for face recognition and clustering. In *Proceedings of the IEEE conference on computer vision and pattern recognition*, pages 815–823, 2015.
  - [44] V. Sharma, M. Tapaswi, M. S. Sarfraz, and R. Stiefelhagen. Self-supervised learning of face representations for video face clustering. In *2019 14th IEEE International Conference on Automatic Face & Gesture Recognition (FG 2019)*, pages 1–8. IEEE, 2019.
  - [45] R. Shyam and Y. N. Singh. Identifying individuals using multimodal face recognition techniques. *Procedia Computer Science*, 48:666–672, 2015.
  - [46] K. Sohn. Improved deep metric learning with multi-class n-pair loss objective. In *Advances in neural information processing systems*, pages 1857–1865, 2016.
  - [47] S. Toshniwal, H. Tang, L. Lu, and K. Livescu. Multitask learning with low-level auxiliary tasks for encoder-decoder based speech recognition. *arXiv preprint arXiv:1704.01631*, 2017.
  - [48] Y.-H. H. Tsai and R. Salakhutdinov. Improving one-shot learning through fusing side information. *arXiv preprint arXiv:1710.08347*, 2017.
  - [49] O. Vinyals, C. Blundell, T. Lillicrap, D. Wierstra, et al. Matching networks for one shot learning. In *Advances in neural information processing systems*, pages 3630–3638, 2016.
  - [50] H. Wang, Y. Wang, Z. Zhou, X. Ji, D. Gong, J. Zhou, Z. Li, and W. Liu. Cosface: Large margin cosine loss for deep face recognition. In *Proceedings of the IEEE conference on computer vision and pattern recognition*, pages 5265–5274, 2018.
  - [51] M. Wang and W. Deng. Mitigating bias in face recognition using skewness-aware reinforcement learning. In *Proceedings of the IEEE/CVF Conference on Computer Vision and Pattern Recognition*, pages 9322–9331, 2020.
  - [52] Y. Wen, K. Zhang, Z. Li, and Y. Qiao. A discriminative feature learning approach for deep face recognition. In *European conference on computer vision*, pages 499–515. Springer, 2016.
  - [53] C. Whitelam, E. Taborsky, A. Blanton, B. Maze, J. Adams, T. Miller, N. Kalka, A. K. Jain, J. A. Duncan, K. Allen, et al. Iarpa janus benchmark-b face dataset. In *proceedings of the IEEE conference on computer vision and pattern recognition workshops*, pages 90–98, 2017.
  - [54] O. Wiles, A. Koepke, and A. Zisserman. Self-supervised learning of a facial attribute embedding from video. *arXiv preprint arXiv:1808.06882*, 2018.
  - [55] L. Wolf, T. Hassner, and I. Maoz. Face recognition in unconstrained videos with matched background similarity. In *CVPR 2011*, pages 529–534. IEEE, 2011.
  - [56] D. Yi, Z. Lei, S. Liao, and S. Z. Li. Deep metric learning for person re-identification. In *2014 22nd International Conference on Pattern Recognition*, pages 34–39. IEEE, 2014.
  - [57] K. Zhang, Z. Zhang, Z. Li, and Y. Qiao. Joint face detection and alignment using multitask cascaded convolutional networks. *IEEE Signal Processing Letters*, 23(10):1499–1503, 2016.